MULTISCALE MODEL. SIMUL.
Vol. 2, No. 4, pp. 662–674

A TWO-SCALE NONPERTURBATIVE APPROACH TO UNCERTAINTY ANALYSIS OF DIFFUSION IN RANDOM COMPOSITES*

DONGBIN XIU† AND DANIEL M. TARTAKOVSKY†

Abstract. Many physical systems, such as natural porous media, are highly heterogeneous and characterized by parameters that are uncertain due to the lack of sufficient data. This uncertainty (randomness) occurs on a multiplicity of scales. We focus on random composites with the two dominant scales of uncertainty: large-scale uncertainty in the spatial arrangement of materials and small-scale uncertainty in the parameters within each material. We propose an approach that combines random domain decompositions and polynomial chaos expansions to account for the large and small scales of uncertainty, respectively. We present a general framework and use one-dimensional diffusion to demonstrate that our combined approach provides robust, nonperturbative approximations for the statistics of system states.

Key words. random fields, moment equations, random domain decomposition, polynomial chaos

AMS subject classifications. 60H30, 86A05, 86A32

DOI. 10.1137/03060268X

1. Introduction.

Simulations of physical processes in most heterogeneous environments are hampered by insufficient parameterization by data. To make predictions under such conditions, one needs to assign the parameter values to the points (cells) on a computational grid, where parameter data are absent. This is commonly done by treating such parameters as random fields, whose statistics are inferred from available data. This renders the governing equations stochastic, even if the underlying physical phenomena are deterministic. While the parameter statistics are often highly non-Gaussian and exhibit nontrivial correlation structures, most stochastic approaches assume the opposite.

Consider, for instance, moment equation approaches, which derive a set of deterministic equations for the statistical moments, usually the ensemble mean and (co)variance, of system states. These approaches require closure approximations, such as perturbation expansions in the variances of system parameters. This formally limits their applicability to mildly heterogeneous environments, i.e., to environments whose parameter variances are small. While such approaches work reasonably well for some nonlinear problems [20], they often fail for others [15].

A nonperturbative alternative to these approaches relies on polynomial chaos expansions. The classical Wiener polynomial chaos [22] defines a span of the Hermite polynomial functionals of a Gaussian process and converges to any L^2 functional in

*Received by the editors December 22, 2003; accepted for publication (in revised form) April 7, 2004; published electronically September 2, 2004. This research was performed under the auspices of the U.S. Department of Energy under contract W-7405-ENG-36. This work was supported in part by the U.S. Department of Energy under the DOE/BES Program in the Applied Mathematical Sciences, contract KC-07-01-01, and by the LDRD Program Office at Los Alamos National Laboratory. This work made use of shared facilities supported by SAHRA (Sustainability of semi-Arid Hydrology and Riparian Areas) under the STC Program of the National Science Foundation under agreement EAR-9876800.

http://www.siam.org/journals/mms/2-4/60268.html

†Theoretical Division, Mathematica Modeling and Analysis Group (T-7), Los Alamos National Laboratory, MS B284, Los Alamos, NM 87545 (xiu@t7.lanl.gov, dmt@lanl.gov).

the L^2 sense [3]. The Wiener chaos has been applied successfully to a variety of engineering applications [10, 11, 12]. Generalizations of the Wiener polynomial chaos are based on fundamental work on stochastic theory [17, 19] and orthogonal polynomials [1, 16] and employ many classes of orthogonal polynomials. These include polynomials from the Askey scheme [1], which is a classification of hypergeometric orthogonal polynomials, and includes the Hermite chaos as a subset. The main advantage of the generalized polynomial chaos is that it can represent many non-Gaussian stochastic processes, including some discrete processes, more efficiently [26, 27, 29]. Mathematical properties of such polynomial expansions applied to stochastic elliptic equations, including their convergence rate, have been analyzed rigorously in [2, 7]. However, as we demonstrate in this study, the generalized polynomial chaos might become computationally inefficient when applied to multimodal processes. The present study is devoted to overcoming this shortcoming.

Our two-scale approach combines the generalized polynomial chaos with the random domain decomposition (RDD) approach [23, 24, 25]. A key advantage of RDD is that it provides robust closures (accurate approximations) of moment equations, even when environments are highly heterogeneous and the statistical distributions and correlation structures of parameters are complex. RDD relies on the fact that a high degree of heterogeneity usually arises from the presence of different materials (populations) in the environment. Specifically, RDD replaces a non-Gaussian, multimodal parameter field $Y(\boldsymbol{x})$ with a two-scale random process. The large-scale randomness arises due to uncertainty in internal boundaries of materials (populations). The small-scale randomness corresponds to uncertainty in parameters within each material. In other words, a non-Gaussian, multimodal probability density function $p_Y(y)$ is replaced with a joint probability density function $p_Y(y,\gamma) = p_Y(y|\gamma)p_\Gamma(\gamma)$. The conditional probability density function $p_Y(y|\gamma)$ describes the distribution of Y within each material conditioned on the boundary location Γ, whose probability density function is $p_\Gamma(\gamma)$. Hence it has convenient properties, such as unimodality and simple correlations.

We start by formulating in section 2 the problem of diffusion in random composite media. We outline the generalized polynomial chaos expansion approach in section 3 and demonstrate its limitations for the multimodal distributions of system parameters. In section 4, we employ a random domain decomposition to extend the range of applicability of polynomial chaos expansions to such parameters. Section 5 provides two computational examples and analyzes the accuracy of the proposed approach.

2. Problem formulation. Consider a state variable h (concentration, temperature, fluid pressure, etc.) whose dynamics are described by the Poisson equation,

$$\nabla \cdot K \nabla h + f = 0. \tag{2.1}$$

The system parameter K (diffusion coefficient, conductivity, permeability, etc.) is sampled at selected locations $\boldsymbol{x}_i$, $i = 1, \ldots, N$, as shown in Figure 1(a). To simplify the presentation, we assume that the source function f and boundary conditions are deterministic. Randomness in these quantities is additive and can be easily incorporated in subsequent analysis [21].

Problem (2.1) is underdetermined, since the values of K at points other than $\{\boldsymbol{x}_i\}$ are unknown. To quantify the uncertainty in K, it is common [5, 30, 6] to treat it as a random field, whose sample statistics, including a correlation structure, are inferred from data. This step relies on the ergodicity hypothesis, which allows one to interchange the ensemble and spatial averages. Figure 1(b) depicts a stationary

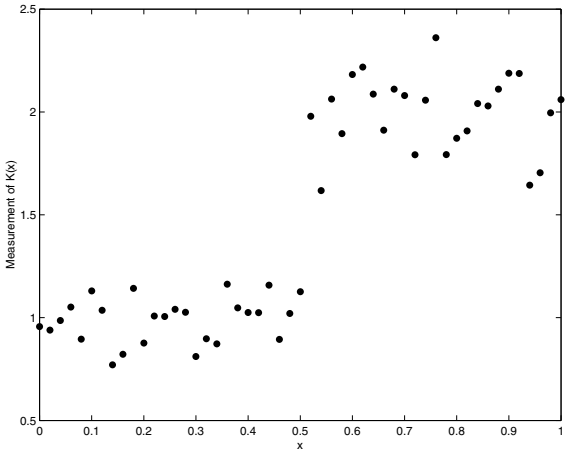

(a)

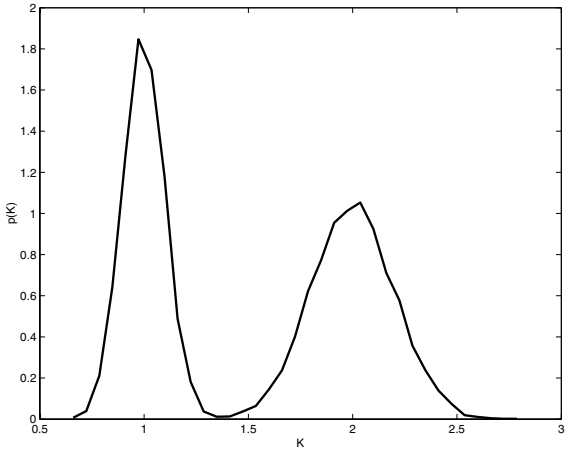

(b)

FIG. 1. (a) *Measurements of conductivity K at selected locations through the one-dimensional medium and* (b) *the corresponding statistically homogeneous probability density function $p(k)$.*

(statistically homogeneous) probability density function, $p(k)$, constructed from the K data in Figure 1(a).

The randomness of K renders (2.1) stochastic, so that its solution is given in terms of the probability density function of h or, equivalently, its ensemble moments. We use the Reynolds decomposition to represent random fields $\mathcal{R} = \langle \mathcal{R} \rangle + \mathcal{R}'$ as the sum of their ensemble means $\langle \mathcal{R} \rangle$ and zero-mean fluctuations $\mathcal{R}'$. Taking the ensemble mean of (2.1) yields the mean equation,

$$\nabla \cdot [\langle K \rangle \nabla \langle h \rangle + \langle K' \nabla h' \rangle] + f = 0, \tag{2.2}$$

that contains the second mixed moment $\langle K' \nabla h' \rangle$, an expression for which is not known. The need to approximate this term is often referred to as a closure problem. One of the most widely used closures relies on perturbation expansions in σ_Y^2, the variances of log conductivity $Y = \ln K$ [5, 9, 4, 6, 18]. This requires the perturbation parameter σ_Y^2 to be small, which is not the case for most multimodal distributions,

such as the one shown in Figure 1(b). Moreover, under certain conditions, the smallness of σ_Y^2 does not guarantee the convergence of perturbation solutions of moment equations [8, 15]. Clearly, there is a need to pursue perturbation-free alternatives to classical moment equation approaches.

The two-scale nonperturbative closure that we introduce here is based on a combination of RDD and polynomial chaos expansion (PCE). RDD is used to decompose the computational domain into subdomains, whose physical parameters have convenient statistical properties, such as unimodality. PCE takes advantage of these properties to compute efficiently and accurately, without resorting to perturbation expansions, the statistics of system states. The main features of this approach are described in the next two sections.

3. Generalized polynomial chaos. The generalized polynomial chaos represents a second-order stochastic process $X(\omega)$, viewed as a function of a random event ω, as

$$X(\omega) = \sum_{j=0}^{\infty} a_j \Phi_j[\boldsymbol{\xi}(\omega)]. \tag{3.1}$$

Here $\{\Phi_j(\boldsymbol{\xi})\}$ are (multidimensional) orthogonal polynomials of the multidimensional random vector $\boldsymbol{\xi}$, which satisfy the orthogonality relation

$$\langle \Phi_i \Phi_j \rangle = \langle \Phi_i^2 \rangle \delta_{ij}, \tag{3.2}$$

where δ_{ij} is the Kronecker delta. The ensemble average of $\Phi_i \Phi_j$ is an inner product in the Hilbert space determined by the support of the random variables,

$$\langle f(\boldsymbol{\xi}) g(\boldsymbol{\xi}) \rangle = \int f(\boldsymbol{\xi}) g(\boldsymbol{\xi}) w(\boldsymbol{\xi}) d\boldsymbol{\xi}, \tag{3.3}$$

with $w(\boldsymbol{\xi})$ denoting a weighting function. In the discrete case, (3.3) takes the form

$$\langle f(\boldsymbol{\xi}) g(\boldsymbol{\xi}) \rangle = \sum_{\boldsymbol{\xi}} f(\boldsymbol{\xi}) g(\boldsymbol{\xi}) w(\boldsymbol{\xi}). \tag{3.4}$$

In (3.1), there is a one-to-one correspondence between the type of orthogonal polynomials $\{\Phi\}$ and the type of random variable $\boldsymbol{\xi}$. The type of orthogonal polynomials $\{\Phi\}$ is chosen in such a way that their weighting function $w(\boldsymbol{\xi})$ in the orthogonality relation (3.3) has the same form as the probability distribution function of the underlying random variable $\boldsymbol{\xi}$. For example, the weighting function of Hermite orthogonal polynomials is $\exp(-\boldsymbol{\xi}^T \boldsymbol{\xi}/2)/\sqrt{(2\pi)^n}$ and is the same as the probability density function of the n-dimensional Gaussian random variable $\boldsymbol{\xi}$. Hence, the classical Wiener polynomial chaos is an expansion of the Hermite polynomials in terms of Gaussian random variables. A few types of the generalized polynomial chaos corresponding to the commonly used distributions are listed in Table 1.

The expansion (3.1) resides in an infinite-dimensional space determined by $\boldsymbol{\xi}$. In practice, the infinite summation in (3.1) has to be truncated. This is achieved by reducing the expansion (3.1) to a finite-dimensional space, i.e., to an expansion of the finite-dimensional random variable $\boldsymbol{\xi}$, according to the nature of random inputs. Additionally, the highest order of polynomials $\{\Phi\}$ is chosen to satisfy accuracy requirements. Thus, (3.1) is approximated by a finite-term expansion,

$$X(\omega) = \sum_{j=0}^{M} a_j \Phi_j(\boldsymbol{\xi}), \tag{3.5}$$

TABLE 1
Correspondence between the type of Wiener–Askey polynomial chaos and its underlying random variables ($N \geq 0$ is a finite integer).

	Random variable $\boldsymbol{\xi}$	Wiener–Askey chaos $\{\Phi(\boldsymbol{\xi})\}$	Support
Continuous	Gaussian	Hermite chaos	$(-\infty, \infty)$
	gamma	Laguerre chaos	$[0, \infty)$
	beta	Jacobi chaos	$[a, b]$
	uniform	Legendre chaos	$[a, b]$
Discrete	Poisson	Charlier chaos	$\{0, 1, 2, \dots\}$
	binomial	Krawtchouk chaos	$\{0, 1, \dots, N\}$
	negative binomial	Meixner chaos	$\{0, 1, 2, \dots\}$
	hypergeometric	Hahn chaos	$\{0, 1, \dots, N\}$

where $\boldsymbol{\xi}$ is an n-dimensional random vector. If the highest order of a polynomial $\{\Phi\}$ is m, then the total number of expansion terms is $(M+1) = (n+m)!/(n!m!)$. Cameron and Martin [3] proved the convergence of Hermite-chaos expansion. For linear elliptic equations, the convergence of general non-Hermite expansions has been demonstrated both numerically [26, 27, 28] and analytically [2].

To demonstrate the robustness of generalized polynomial chaos expansions, we consider a highly non-Gaussian unimodal random variable $X = 1+B(1,6)+N(0,4)+5U(0,1)+E(3)$, where $B(1,6)$ is a β random variable with parameters $\alpha = 1$ and $\beta = 6$, $N(0,4)$ is a Gaussian random variable with zero-mean and standard deviation 4, $U(0,1)$ is a uniform random variable in $(0,1)$, and $E(3)$ is an exponential random variable with mean 3. The variance of X is $\sigma_X^2 = 26.8$, which clearly disqualifies it as a small parameter in perturbation expansions. On the other hand, Figure 2(a) demonstrates that the fifth-degree Hermite polynomial is sufficient to accurately approximate this distribution.

The situation is radically different when one deals with system parameters that are neither Gaussian nor unimodal. Figure 2(b) demonstrates that the Hermite polynomials are not adequate to represent the bimodal cumulative density function corresponding to $p(k)$ shown in Figure 1(b).

4. Random domain decomposition. To apply the generalized polynomial chaos expansions to systems whose parameters are multimodal, we reformulate the problem (2.1) in terms of the random domain decomposition [23, 24]. Within this framework, the randomness of $K(\boldsymbol{x})$ stems from two factors: large-scale uncertainty in the spatial arrangement of N subdomains $\{\Omega_i\}_{i=1}^N$ (or, equivalently, the boundaries $\{\Gamma_{ij}\}$ between subdomains Ω_i and Ω_j for $i \neq j$) and small-scale uncertainty in K within each subdomain. Then $p_K(k)$, the probability density function of K, is replaced with a joint probability density function $p_K(k,\gamma) = p_K(k|\gamma)p_\Gamma(\gamma)$.

The reconstruction of $p_\Gamma(\gamma)$, the probability density function of a random boundary Γ, from measurements of $K(\boldsymbol{x})$ is a subject of an ongoing research [14], which we do not pursue here. The reverse relationship, however, is more straightforward. Indeed, if p_{K_i} are the probability density functions of $K = K_i$ within each random subdomain Ω_i, then the probability density function of the mixture is

$$p_K(k;\boldsymbol{x}) = \sum_i P_i(\boldsymbol{x}) p_{K_i}(k), \tag{4.1}$$

where $P_i(\boldsymbol{x})$ is the probability that $\boldsymbol{x} \in \Omega_i$, which is uniquely defined by $p_\Gamma(\gamma)$.

Let $K(\boldsymbol{x}) = K_i(\boldsymbol{x})\mathbb{I}_{\Omega_i}(\boldsymbol{x})$, where $\mathbb{I}_{\Omega_i}(\boldsymbol{x})$ is the indicator function. Then (2.1) can

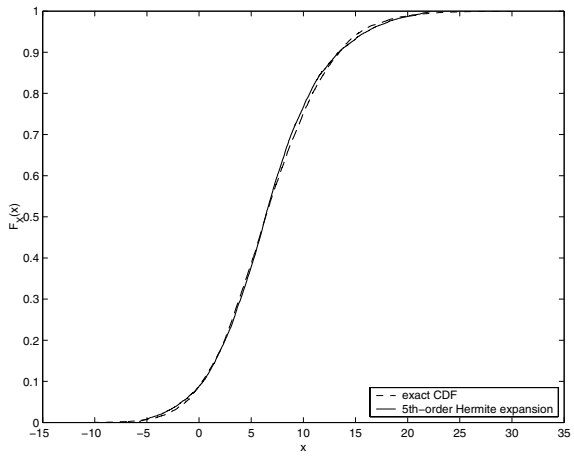

(a)

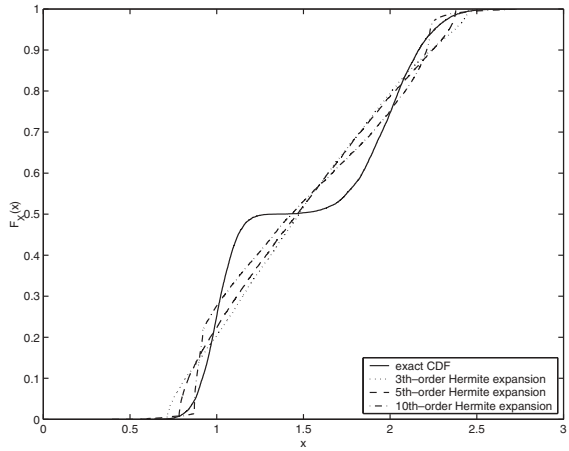

(b)

FIG. 2. *The Hermite expansions for the cumulative distribution functions of* (a) *a highly non-Gaussian but unimodal random process and* (b) *a bimodal process corresponding to the data in Figure* 1.

be rewritten as

$$\nabla \cdot K_i \nabla h(\boldsymbol{x}) + f = 0, \qquad \boldsymbol{x} \in \Omega_i, \qquad i = 1, \ldots, N. \tag{4.2}$$

Boundary conditions for (2.1) are supplemented by the conditions of the continuity of both the random state variable, h, and the normal component of $\boldsymbol{q}_{ij} = -K\nabla h$, the random flux across the random boundaries Γ_{ij} $\forall i \neq j$. Previous one- and two-dimensional applications of RDD involved both regular (a contact point in one dimension [24], as well as a contact line [13] and a square inclusion [25] in two dimensions) and irregular (as inferred from actual field data [14]) random boundaries. In these applications, RDD was combined with perturbation closures, whose limitations we discussed in the introduction.

Here generalized polynomial chaos expansions, rather than perturbation expansions, are applied to the relevant random fields within each subdomain, and the resulting probability density function of h is matched along the random boundaries Γ_{ij} $\forall i \neq j$. To simplify presentation, we consider a two-subdomain problem $\Omega = \Omega_1 \cup \Omega_2$ and denote the boundary between these two subdomains by $\Gamma = \Gamma_{12}$.

4.1. Conditional statistics. The first step of the averaging procedure consists of the use of polynomial chaos expansions within each subdomain Ω_i $(i = 1, 2)$,

$$h_i(x) = \sum_{m=0}^{M} \hat{h}_{i,m}\Phi_m(\boldsymbol{\xi}) \quad \text{and} \quad K_i(x) = \sum_{m=0}^{M} \hat{K}_{i,m}\Phi_m(\boldsymbol{\xi}), \quad \text{for } x \in \Omega_i. \tag{4.3}$$

Inserting these expansions into (4.2) and using a Galerkin projection onto each basis of $\{\Phi_m\}_{m=0}^{M}$ yields

$$\sum_{m=0}^{M}\sum_{n=0}^{M} \nabla \cdot \hat{K}_{i,m}\nabla\hat{h}_{i,n}\langle\Phi_m\Phi_n\Phi_l\rangle + f_i\delta_{l0} = 0, \qquad i = 1, 2. \tag{4.4}$$

Here we assume the source function f to be deterministic. A random f can be treated as well by expanding it in a series analogous to (4.3). Denoting $H_i = [\hat{h}_{i,0}, \dots, \hat{h}_{i,M}]^T$ and $F_i = [f_i, 0, \dots]^T$ allows us to rewrite (4.4) in a matrix form,

$$\nabla \cdot B_i^T \nabla H_i + F_i = 0, \qquad i = 1, 2, \tag{4.5}$$

where $B_i(x) = [b_{i,nl}]_{n,l=0}^{M}$ is a symmetric matrix of size $(M + 1) \times (M + 1)$, whose entries are

$$b_{i,nl} = \sum_{m=0}^{M} \hat{K}_{i,m}\langle\Phi_m\Phi_n\Phi_l\rangle, \qquad i = 1, 2. \tag{4.6}$$

The continuity of head and flux along the random boundary Γ,

$$h|_{x=\Gamma^-} = h|_{x=\Gamma^+}, \qquad K(x)\frac{dh}{dx}\bigg|_{x=\Gamma^-} = K(x)\frac{dh}{dx}\bigg|_{x=\Gamma^+},$$

gives rise to

$$H_1|_{x=\Gamma^-} = H_2|_{x=\Gamma^+}, \qquad B_1^T\frac{dH_1}{dx}\bigg|_{x=\Gamma^-} = B_2^T\frac{dH_2}{dx}\bigg|_{x=\Gamma^+}. \tag{4.7}$$

Equation (4.5), together with (4.7) and external boundary conditions, defines a complete system of algebraic equations for h conditioned on the random interface Γ. The conditional statistics of h can be readily obtained upon solving this system, e.g., $\langle h(x)|\Gamma\rangle = \hat{h}_0(x)$, $\sigma_h^2|\Gamma = \sum_{m=1}^{M} \hat{h}_m^2(x)\langle\Phi_m^2\rangle$.

4.2. Averaging over geometries. In the second step, the statistics of h are obtained by averaging the conditional statistics of h over the random geometry Γ, e.g.,

$$\begin{aligned}\langle h(x)\rangle &= \iint h(x;k,\gamma)p(k,\gamma)dkd\gamma = \iint h(x;k,\gamma)p(k|\gamma)p_\Gamma(\gamma)dkd\gamma \\ &= \int \langle h(x)|\gamma\rangle p_\Gamma(\gamma)d\gamma.\end{aligned} \tag{4.8}$$

To evaluate the above integral, we employ a quadrature rule,

$$\langle h(x)\rangle = \sum_{q=1}^{Q}\langle h(x)|\alpha_q\rangle w_q. \tag{4.9}$$

Here $\{\alpha_q, w_q\}_{q=1}^{Q}$ are quadrature points and the corresponding weights of the orthogonal polynomials $g_Q(\gamma)$, respectively. The orthogonality condition gives

$$\int g_m(\gamma)g_n(\gamma)p_\Gamma(\gamma)d\gamma = d_m^2\delta_{mn}.$$

For example, if Γ can be parameterized by either Gaussian or uniformly distributed random variables, $\{g_m\}$ take, respectively, the form of either the Hermite or Legendre polynomials. Expressions for σ_h^2 and other higher-order statistics can be obtained in a similar manner.

5. Computational examples. To simplify the presentation, we consider the one-dimensional version of (2.1) defined on $\Omega = (0,1)$ and set $f = 0$. This equation is subject to the boundary conditions $q(0) = q_0$ and $h(1) = 0$. Two examples are considered.

5.1. Random contact point. In the first example, the random materials $[0,\alpha)$ and $(\alpha,1]$ are joined at the random location α. Then $p_K(k)$, the probability density function of K shown in Figure 1(b), is replaced with a joint probability density function $p_K(k,\alpha) = p_K(k|\alpha)p_\alpha(\alpha)$. We assume that $Y_i = \ln K_i(x)$ are mutually uncorrelated Gaussian random fields with exponential correlation functions and that α is either a (a) truncated Gaussian or (b) uniformly distributed random variable.

This problem admits an analytical solution for random h,

$$h(x) \;=\; q_0\mathcal{H}(\alpha - x)\left[\int_x^\alpha \frac{ds}{K_1(s)} \;+\; \int_\alpha^1 \frac{ds}{K_2(s)}\right] \;+\; q_0\mathcal{H}(x-\alpha)\int_x^1 \frac{ds}{K_2(s)}, \tag{5.1}$$

where $\mathcal{H}(z)$ is the Heaviside function,

$$\mathcal{H}(z) = \begin{cases} 1, & z \ge 0, \\ 0, & z < 0. \end{cases} \tag{5.2}$$

For Gaussian α and arbitrary correlation functions of Y_i, taking the ensemble average of (5.1) gives an exact solution for the mean,

$$\begin{aligned}\frac{\langle h(x)\rangle}{q_0} &= \frac{\sqrt{2}\,\sigma_\alpha}{\sqrt{\pi}\,\mathcal{W}}\left[\frac{1}{K_{H_1}} - \frac{1}{K_{H_2}}\right]\left[e^{-u^2} - e^{-u_1^2}\right] - \frac{\langle\alpha\rangle - x}{\mathcal{W}}\left[\frac{1}{K_{H_1}} - \frac{1}{K_{H_2}}\right]\operatorname{erf}(u) \\ &+ \frac{1}{\mathcal{W}}\left[\frac{\langle\alpha\rangle - x}{K_{H_1}} + \frac{1-\langle\alpha\rangle}{K_{H_2}}\right]\operatorname{erf}(u_1) - \frac{1}{\mathcal{W}}\frac{1-x}{K_{H_2}}\operatorname{erf}(u_0),\end{aligned} \tag{5.3}$$

where $K_{H_i} = K_{G_i}\exp(\sigma_{Y_i}^2/2)$ are the harmonic means of the $K_i(x)$ fields, $K_{G_i} =$

$\exp(\langle Y_i \rangle)$ are their geometric means, and

(5.4)
$$u = \frac{x - \langle \alpha \rangle}{\sqrt{2}\sigma_\alpha}, \qquad u_0 = -\frac{\langle \alpha \rangle}{\sqrt{2}\sigma_\alpha}, \qquad u_1 = \frac{1 - \langle \alpha \rangle}{\sqrt{2}\sigma_\alpha}, \qquad \mathcal{W} = \operatorname{erf}(u_1) - \operatorname{erf}(u_0).$$

Assuming the exponential covariance functions, $C_{Y_i}(x, y) = \sigma_{Y_i}^2 \exp(- \mid x - y \mid / l_{Y_i})$, where l_{Y_i} is the correlation length of the ith material, (5.1) gives an exact expression for the variance,

$$\begin{aligned}
\frac{\sigma_h^2(x)}{q_0} &= 2\frac{\sigma_{Y_1}^2 l_{Y_1}^2}{\mathcal{W} K_{G_1}^2} \left\{ \left[\frac{\langle \alpha \rangle - x}{l_{Y_1}} - 1 \right] [\operatorname{erf}(u_1) - \operatorname{erf}(u)] + \sqrt{\frac{2}{\pi}} \frac{\sigma_\alpha}{l_{Y_1}} \left[e^{-u^2} - e^{-u_1^2} \right] \right. \\
&\qquad \left. + \exp\left(\frac{x - \langle \alpha \rangle}{l_{Y_1}} + \frac{\sigma_\alpha^2}{2 l_{Y_1}^2} \right) \left[\operatorname{erf}\left(u_1 + \frac{\sigma_\alpha}{\sqrt{2} l_{Y_1}} \right) - \operatorname{erf}\left(u + \frac{\sigma_\alpha}{\sqrt{2} l_{Y_1}} \right) \right] \right\} \\
&\quad + 2\frac{\sigma_{Y_2}^2 l_{Y_2}^2}{\mathcal{W} K_{G_2}^2} \left\{ \left[\frac{1 - \langle \alpha \rangle}{l_{Y_2}} - 1 \right] [\operatorname{erf}(u_1) - \operatorname{erf}(u)] - \sqrt{\frac{2}{\pi}} \frac{\sigma_\alpha}{l_{Y_2}} \left[e^{-u^2} - e^{-u_1^2} \right] \right. \\
&\qquad \left. + \exp\left(\frac{\langle \alpha \rangle - 1}{l_{Y_2}} + \frac{\sigma_\alpha^2}{2 l_{Y_1}^2} \right) \left[\operatorname{erf}\left(u_1 - \frac{\sigma_\alpha}{\sqrt{2} l_{Y_1}} \right) - \operatorname{erf}\left(u - \frac{\sigma_\alpha}{\sqrt{2} l_{Y_1}} \right) \right] \right\} \\
&\quad + 2\frac{\sigma_{Y_2}^2 l_{Y_2}^2}{\mathcal{W} K_{G_2}^2} \left[\frac{1 - x}{l_{Y_2}} + e^{(x-1)/l_{Y_2}} - 1 \right] [\operatorname{erf}(u) - \operatorname{erf}(u_0)] . \qquad (5.5)
\end{aligned}$$

Exact expressions for $\langle h \rangle$ and σ_h^2 corresponding to the uniformly distributed α are derived from (5.1) in a similar manner.

Figure 3 demonstrates that the ensemble mean, $\langle h \rangle$, and standard deviation, σ_h, of h computed with the RDD-PCE approach outlined in section 4 practically coincide with their exact counterparts given by (5.3) and (5.5), respectively. The first 20 terms are retained in the polynomial expansion. In these calculations, we set $Y_1(x) = N(0, 0.1)$, $Y_2(x) = N(2, 0.2)$, $l_{Y_1} = 5$, $l_{Y_2} = 1$, and $q_0 = 1$, and we approximate the truncated Gaussian α with $\alpha = N(0.5, 0.05)$.

To examine the accuracy and convergence of our RDD-PCE approach, we plot in Figure 4 the error introduced by approximating (4.8) with (4.9) as a function of the number of quadrature points. To isolate errors introduced by (4.9), we fix the PCE expansion at third order and employ a sufficient resolution of the spatial discretization in a finite-difference method. Figure 4 shows a nearly exponential convergence rate for the number of quadratures up to 4. Truncation of the tails of the Gaussian distribution of α introduces an additional small error term, which accounts for the deviation from the exponential convergence for the larger number of quadratures. Since the uniformly distributed α does not require any truncation approximations, it results in the error convergence that is close to exponential (Figure 4). In these calculations, we set $\alpha \sim U(-0.45, 0.55)$. Such an exponential error convergence is in line with the earlier theoretical [2] and numerical [26] findings.

5.2. Random inclusion. In the second example, an inclusion of the width 1/3 and random conductivity K_2 is embedded in the material of random conductivity K_1. The location of the inclusion, as characterized by its center α, is random. The statistics of K_1, K_2, and α are the same as in the previous example.

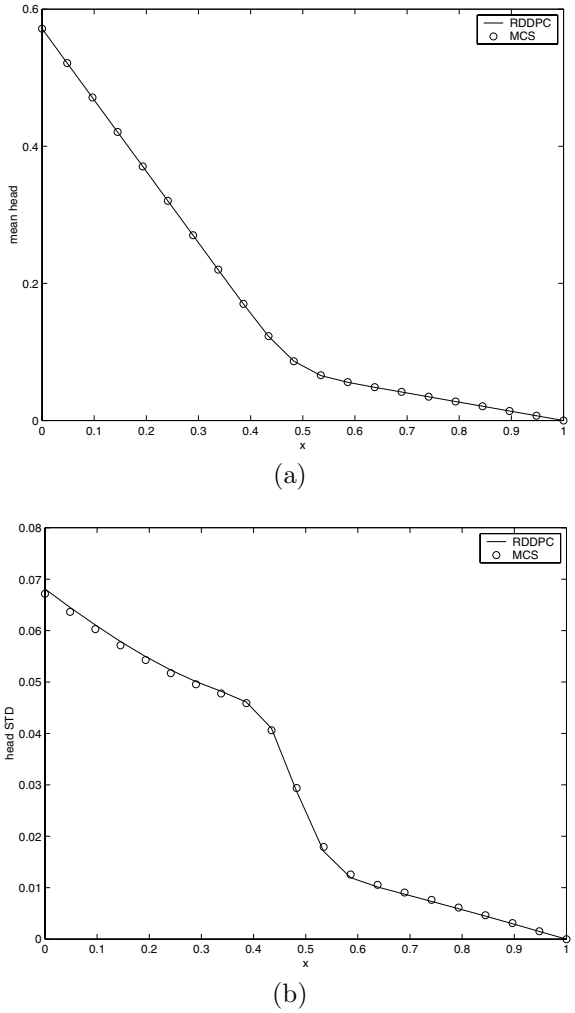

FIG. 3. *The ensemble mean* (a) *and standard deviation* (b) *of h given by the exact analytical solutions (circles) and by the polynomial chaos expansion (solid lines).*

In this case, we compare the h statistics computed by a low-order polynomial chaos expansion with those obtained from 2000 Monte Carlo simulations. Figure 5 shows that just five terms in the polynomial chaos expansion are enough to calculate accurately the ensemble mean, $\langle h \rangle$, and standard deviation, σ_h, of h.

6. Conclusions. Polynomial chaos expansions provide a valuable tool for quantifying uncertainty in physical systems with uncertain (random) system parameters. However, they might become less efficient if these parameter have highly non-Gaussian, multimodal distributions and/or short correlation lengths. To extend the range of applicability of the PCE approaches, we combined them with a random domain decomposition. We used one-dimensional diffusion to demonstrate that this combined approach provides robust, perturbation-free approximations for the statistics of the system states.

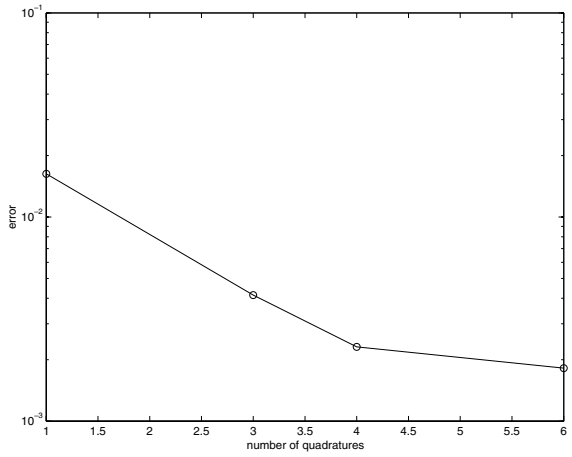

(a)

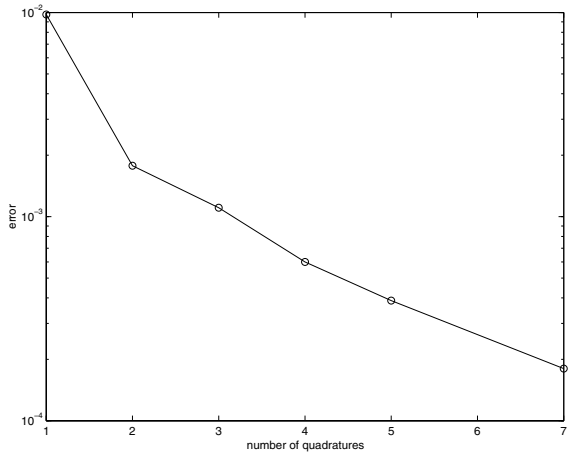

(b)

FIG. 4. *The error convergence of* $\langle h \rangle$ *for the* (a) *Gaussian and* (b) *uniformly distributed contact point* α.

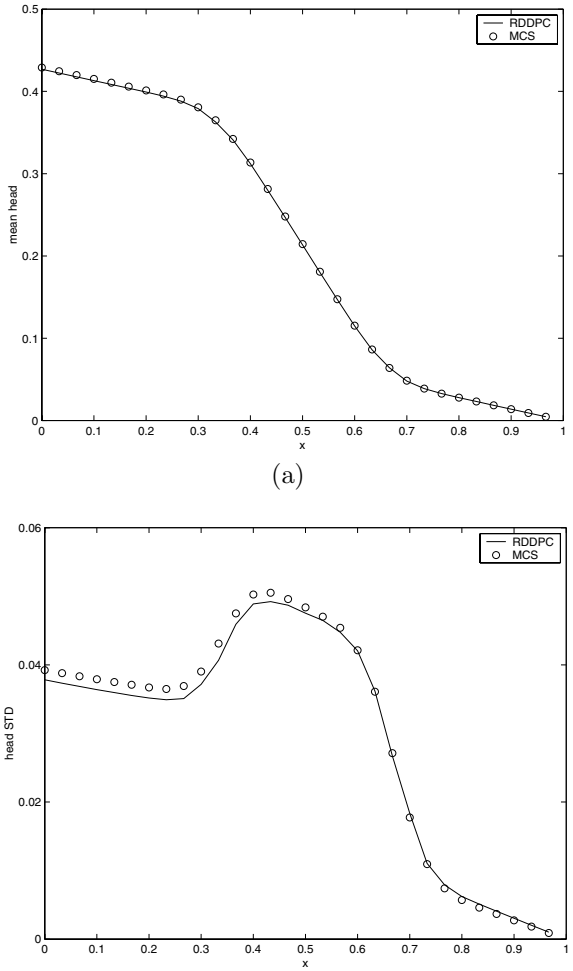

FIG. 5. *The ensemble mean* (a) *and standard deviation* (b) *of h computed with the RDD-PCE approach (solid lines) and Monte Carlo simulations (circles).*

Acknowledgment. The authors thank the anonymous reviewers for their valuable comments and suggestions.

REFERENCES

[1] R. ASKEY AND J. WILSON, *Some Basic Hypergeometric Polynomials that Generalize Jacobi Polynomials*, Mem. Amer. Math. Soc. 319, AMS, Providence, RI, 1995.
[2] I. BABUŠKA, R. TEMPONE, AND G. ZOURARIS, *Galerkin Finite Element Approximations of Stochastic Elliptic Differential Equations*, Tech. report 02-38, TICAM, Austin, TX, 2002.
[3] R. CAMERON AND W. MARTIN, *The orthogonal development of nonlinear functionals in series of Fourier-Hermite functionals*, Ann. of Math. (2), 48 (1947), pp. 385–392.
[4] J. H. CUSHMAN, *The Physics of Fluids in Hierarchical Porous Media: Angstroms to Miles*, Kluwer Academic Publishers, New York, 1997.
[5] G. DAGAN, *Flow and Transport in Porous Formations*, Springer-Verlag, New York, 1989.
[6] G. DAGAN AND S. P. NEUMAN, EDS., *Subsurface Flow and Transport: A Stochastic Approach*, Cambridge University Press, New York, 1997.

[7] M. Deb, I. Babuška, and J. Oden, *Solution of stochastic partial differential equations using Galerkin finite element techniques*, Comput. Methods Appl. Mech. Engrg., 190 (2001), pp. 6359–6372.
[8] U. Frisch, *Wave propagation in random media*, in Probabilistic Methods in Applied Mathematics, Vol. 1, A. T. Bharucha-Reid, ed., Academic Press, New York, 1968, pp. 75–198.
[9] L. W. Gelhar, *Stochastic Subsurface Hydrology*, Prentice–Hall, Englewood Cliffs, NJ, 1993.
[10] R. Ghanem, *Scales of fluctuation and the propagation of uncertainty in random porous media*, Water Resour. Res., 34 (1998), p. 2123.
[11] R. Ghanem, *Stochastic finite elements for heterogeneous media with multiple random non-Gaussian properties*, ASCE J. Eng. Mech., 125 (1999), pp. 26–40.
[12] R. Ghanem and P. Spanos, *Stochastic Finite Elements: A Spectral Approach*, Springer-Verlag, New York, 1991.
[13] A. Guadagnini, L. Guadagnini, D. M. Tartakovsky, and C. L. Winter, *Random domain decomposition for flow in heterogeneous stratified aquifers*, Stochastic Environ. Res. and Risk Assessment (SERRA), 17 (2003), pp. 394–407.
[14] L. Guadagnini, A. Guadagnini, and D. M. Tartakovsky, *Probabilistic reconstruction of geologic facies*, J. Hydrol., 294 (2004), pp. 57–67.
[15] K. D. Jarman and T. F. Russell, *Eulerian moment equations for stochastic immiscible flow*, Multiscale Model. Simul., 1 (2003), pp. 598–608.
[16] R. Koekoek and R. Swarttouw, *The Askey-Scheme of Hypergeometric Orthogonal Polynomials and Its q-Analogue*, Tech. report 98-17, Department of Technical Mathematics and Informatics, Delft University of Technology, Delft, The Netherlands, 1998.
[17] H. Ogura, *Orthogonal functionals of the Poisson process*, IEEE Trans. Information Theory, 18 (1972), pp. 473–481.
[18] Y. Rubin, *Applied Stochastic Hydrogeology*, Oxford University Press, New York, 2003.
[19] W. Schoutens, *Stochastic Processes in the Askey Scheme*, Ph.D. thesis, K. U. Leuven, Leuven, The Netherlands, 1999.
[20] D. M. Tartakovsky, A. Guadagnini, and M. Riva, *Stochastic averaging of nonlinear flows in heterogeneous porous media*, J. Fluid Mech., 492 (2003), pp. 47–62.
[21] D. M. Tartakovsky and S. P. Neuman, *Extension of "Transient flow in bounded randomly heterogeneous domains* 1. *Exact conditional moment equations and recursive approximations,"* Water Resour. Res., 35 (1999), pp. 1921–1925.
[22] N. Wiener, *The homogeneous chaos*, Amer. J. Math., 60 (1938), pp. 897–936.
[23] C. L. Winter and D. M. Tartakovsky, *Mean flow in composite porous media*, Geophys. Res. Lett., 27 (2000), pp. 1759–1762.
[24] C. L. Winter and D. M. Tartakovsky, *Groundwater flow in heterogeneous composite aquifers*, Water Resour. Res., 38 (2002), doi:10.1029/2001WR000450.
[25] C. L. Winter, D. M. Tartakovsky, and A. Guadagnini, *Numerical solutions of moment equations for flow in heterogeneous composite aquifers*, Water Resour. Res., 38 (2002), doi:10.1029/2001WR000222.
[26] D. Xiu and G. Karniadakis, *Modeling uncertainty in steady state diffusion problems via generalized polynomial chaos*, Comput. Methods Appl. Math. Engrg., 191 (2002), pp. 4927–4948.
[27] D. Xiu and G. Karniadakis, *The Wiener–Askey polynomial chaos for stochastic differential equations*, SIAM J. Sci. Comput., 24 (2002), pp. 619–644.
[28] D. Xiu and G. Karniadakis, *Modeling uncertainty in flow simulations via generalized polynomial chaos*, J. Comput. Phys., 187 (2003), pp. 137–167.
[29] D. Xiu and G. Karniadakis, *A new stochastic approach to transient heat conduction modeling with uncertainty*, Inter. J. Heat Mass Trans., 46 (2003), pp. 4681–4693.
[30] A. M. Yaglom, *Correlation Theory of Stationary and Related Random Functions.* I. *Basic Results*, Springer-Verlag, New York, 1987.